CLUSTERING OF DUST-OBSCURED GALAXIES AT $z \sim 2$

MARK BRODWIN,[1] ARJUN DEY,[1] MICHAEL J. I. BROWN,[2] ALEXANDRA POPE,[1] LEE ARMUS,[3] SHANE BUSSMANN,[1]
VANDANA DESAI,[3] BUELL T. JANNUZI,[1] AND EMERIC LE FLOC'H[4]

ABSTRACT

We present the angular autocorrelation function of 2603 dust-obscured galaxies (DOGs) in the Boötes field of the NOAO Deep Wide-Field Survey. DOGs are red, obscured galaxies, defined as having $R - [24] \geq 14$ ($F_{24}/F_R \gtrsim 1000$). Spectroscopy indicates that they are located at $1.5 \lesssim z \lesssim 2.5$. We find strong clustering, with $r_0 = 7.40^{+1.27}_{-0.84} \, h^{-1}$ Mpc for the full $F_{24} > 0.3$ mJy sample. The clustering and space density of the DOGs are consistent with those of submillimeter galaxies, suggestive of a connection between these populations. We find evidence for luminosity-dependent clustering, with the correlation length increasing to $r_0 = 12.97^{+4.26}_{-2.64} \, h^{-1}$ Mpc for brighter ($F_{24} > 0.6$ mJy) DOGs. Bright DOGs also reside in richer environments than fainter ones, suggesting these subsamples may not be drawn from the same parent population. The clustering amplitudes imply average halo masses of $\log M = 12.2^{+0.3}_{-0.2} \, M_\odot$ for the full DOG sample, rising to $\log M = 13.0^{+0.4}_{-0.3} \, M_\odot$ for brighter DOGs. In a biased structure formation scenario, the full DOG sample will, on average, evolve into $\sim 3 L_*$ present-day galaxies, whereas the most luminous DOGs may evolve into brightest cluster galaxies.

Subject headings: galaxies: evolution — galaxies: formation — galaxies: high-redshift — galaxies: statistics — large-scale structure of universe

1. INTRODUCTION

The bulk of the stellar mass in the universe is created at $1 < z < 3$ (e.g., Dickinson et al. 2003; Rudnick et al. 2006). At $z \approx 1$ this enhanced star formation occurs primarily in luminous infrared galaxies (LIRGs; $10^{11} \leq L_{IR} \, (L_\odot) < 10^{12}$) (Le Floc'h et al. 2005), and by $z \approx 2$ LIRGs and ultraluminous infrared galaxies (ULIRGs; $L_{IR} \, (L_\odot) \geq 10^{12}$) dominate the star formation rate (SFR) budget (e.g., Caputi et al. 2007). Studies of the spatial distribution of subsets of the $1 < z < 3$ ULIRG population with red optical to mid-IR colors have found very strong clustering (Farrah et al. 2006; Magliocchetti et al. 2008), spanning the range seen from $z \sim 2$ submillimeter galaxies (SMGs; Blain et al. 2004) to high-redshift $z \gtrsim 1$ clusters (Brodwin et al. 2007).

Dey et al. (2008, hereafter D08; see also Fiore et al. 2008) presented a sample of IR-luminous dust-obscured galaxies (DOGs) selected via a simple optical/mid-IR color cut. The space density and redshift distribution of these DOGs are similar to those of submillimeter selected galaxies (Chapman et al. 2005; Coppin et al. 2006). Studies of the spectral energy distributions (SEDs) of DOG samples show they contain both starburst- and AGN-dominated galaxies, with the AGN fraction increasing with luminosity. Bright ($F_{24} \approx 1$ mJy) DOGs in Boötes have SEDs of warm AGN ULIRGs (Tyler et al. 2008), whereas the majority of faint ($F_{24} > 0.1$ mJy; $\langle F_{24} \rangle = 0.18$ mJy)[5] DOGs in the GOODS-N field are dominated by star formation (Pope et al. 2008b, hereafter P08). In this Letter, we study the clustering and environment of DOGs as a function of luminosity to explore their role in galaxy formation at the key $z \sim 2$ epoch.

We use a concordance cosmology with $\Omega_M = 0.3$ and $\Omega_\Lambda = 0.7$. Magnitudes are Vega-relative. We report correlation lengths in units of comoving h^{-1} Mpc, with $H_0 = 100 \, h$ km s^{-1} Mpc^{-1}. All other physical quantities assume $h = 0.7$.

2. DUST-OBSCURED GALAXIES

We study the DOG sample presented by D08. DOGs were identified in the Boötes field of the NOAO Deep Wide-Field Survey (NDWFS;[6] Jannuzi & Dey 1999) via a simple optical/ infrared color selection: $R - [24] > 14$, or equivalently, $F_{24}/F_R \gtrsim 1000$. Down to a flux density limit of $F_{24} > 0.3$ mJy ($\approx 6 \, \sigma$) 2603 sources satisfy this criterion in 8.140 deg^2 in Boötes. Spectroscopy (Houck et al. 2005; Weedman et al. 2005; Brand et al. 2007; Desai et al. 2008a, 2008b) of 86 DOGs indicate that they lie in a relatively narrow range of redshifts, well parameterized by a Gaussian with $\bar{z} = 1.99$ and $\sigma = 0.45$ (D08).

3. CLUSTERING OF DOGs

The angular autocorrelation function (ACF) of DOGs is computed as a function of apparent brightness. Given the narrow range of redshifts (Fig. 7 of D08), this binning by flux density is to good approximation a probe of the luminosity dependence of the clustering.

The ACF, parameterized as a simple power law, $\omega(\theta) = A_\omega \theta^{-\delta}$, can be deprojected (Limber 1954) to yield a measurement of the real-space correlation length, $r_0(z)$, over the redshift range spanned by the 2D sample:

$$r_0^\gamma(z) = A_\omega \left\{ \frac{H_0 H_\gamma}{c} \frac{\int_{z_1}^{z_2} N^2(z) \, [x(z)]^{1-\gamma} \, E(z) \, dz}{[\int_{z_1}^{z_2} N(z) \, dz]^2} \right\}^{-1}. \quad (1)$$

Here $\gamma \equiv 1 + \delta$, $H_\gamma = \Gamma(1/2) \, \Gamma[(\gamma - 1)/2]/\Gamma(\gamma/2)$, $N(z)$ is the redshift distribution, and $E(z)$ and $x(z)$ describe the evolution of the Hubble parameter and the comoving radial distance, respectively. The primary uncertainty in the inferred real-space correlation length comes from uncertainty in the shape of the redshift distribution.

[1] NOAO, 950 North Cherry Avenue, Tucson, AZ 85719.
[2] School of Physics, Monash University, Clayton 3800, Victoria, Australia.
[3] *Spitzer* Science Center, California Institute of Technology, Pasadena, CA 91125.
[4] Institute for Astronomy, University of Hawaii, Honolulu, HI 96822.
[5] Angle brackets refer to median values.

[6] See also http://www.noao.edu/noao/noaodeep/.

F_{24} (mJy)	$\langle F_{24} \rangle$ (mJy)	N	$r_0{}^a$ (h^{-1} Mpc)	b	Halo Mass log $(M/M_\odot)$	$L/L_*(z = 0)$
>0.3	0.40	2603	$7.40 \pm^{1.27}_{0.84}$	$3.12 \pm^{0.51}_{0.34}$	$12.2 \pm^{0.3}_{0.2}$	$3.4 \pm^{0.5}_{0.7}$
0.3–0.5	0.36	1846	$7.99 \pm^{1.41}_{1.30}$	$3.36 \pm^{0.56}_{0.52}$	$12.3 \pm^{0.2}_{0.3}$	$3.7 \pm^{0.8}_{0.8}$
>0.4	0.53	1285	$8.66 \pm^{1.41}_{2.10}$	$3.63 \pm^{0.56}_{0.84}$	$12.5 \pm^{0.2}_{0.4}$	$4.1 \pm^{1.2}_{0.8}$
>0.5	0.65	757	$10.19 \pm^{2.47}_{2.64}$	$4.24 \pm^{0.97}_{1.05}$	$12.7 \pm^{0.3}_{0.5}$	$5.0 \pm^{1.5}_{1.4}$
>0.6	0.85	454	$12.97 \pm^{4.26}_{2.64}$	$5.33 \pm^{1.65}_{1.04}$	$13.0 \pm^{0.4}_{0.3}$	$6.6 \pm^{1.5}_{2.4}$

NOTES.—F_{24} is the 24 μm flux density, N refers to the total numbers of sources in each flux bin, and b is the linear bias. Masses and luminosities assume $h = 0.7$.

^{a} Correlation length from the Bayesian fit. The uncertainty range corresponds to the 68% confidence interval.

We calculate the ACF using the Hamilton (1993) estimator:

$$\omega_H = \frac{DD \times RR}{DR \times DR} - 1. \qquad (2)$$

Here DD, DR, and RR are the sum of ordered data-data, data-random, and random-random pairs at each angular separation. We used 500,000 randoms to ensure a robust Monte Carlo integration. We also computed the ACF using the Landy & Szalay (1993) estimator and find nearly identical results.

Regions of the survey affected by cosmetic artifacts or data quality issues can compromise a robust measurement of clustering. Masking is implemented in the images and random catalogs to reject these areas.

A Bayesian technique is used to determine the correlation lengths. This allows marginalization over the slope, δ, subject to the weak prior that $0.2 \leq \delta \leq 1.8$. This is desirable since the small size of some of the subsamples precludes precise simultaneous measurements of both the amplitude and the slope. We show in Figure 1 the simple χ^2 fits and the Bayesian likelihood functions in r_0 computed using the redshift distribution from D08. The slopes in the χ^2 fits for all samples are consistent with $\delta = 0.9$. Results are summarized in Table 1.

The ACF errors were derived using the full covariance matrix, computed using the Brown et al. (2008) implementation of the Eisenstein & Zaldarriaga (2001) analytic approximation. Conservatively assuming 5% of the DOG sample is spurious and uncorrelated, then at most we are underestimating the clustering by ≈11%.

We show in Figure 2 the correlation length versus median flux density for several DOG subsamples. For comparison we also show the 1 σ range for the Blain et al. (2004) SMG sample. The trend is strongly suggestive of luminosity-dependent DOG clustering which, as a consequence, implies that bright and faint DOGs must reside in different environments. We show below (§ 4) that this is observed. While the uncertainties preclude ruling out the null hypothesis of no luminosity dependence from the clustering measurements alone, the clustering and environmental studies, taken together, provide convincing evidence of an intrinsic difference between bright and faint DOGs.

The primary uncertainty in Limber inversion is the sample redshift distribution. If the assumed distribution is broader than the true distribution the resulting amplitudes will be biased high. Our DOG redshift distribution is based on 86 spectroscopic redshifts, drawn largely from the bright end of the DOG population, and may not be representative of the fainter DOGs.
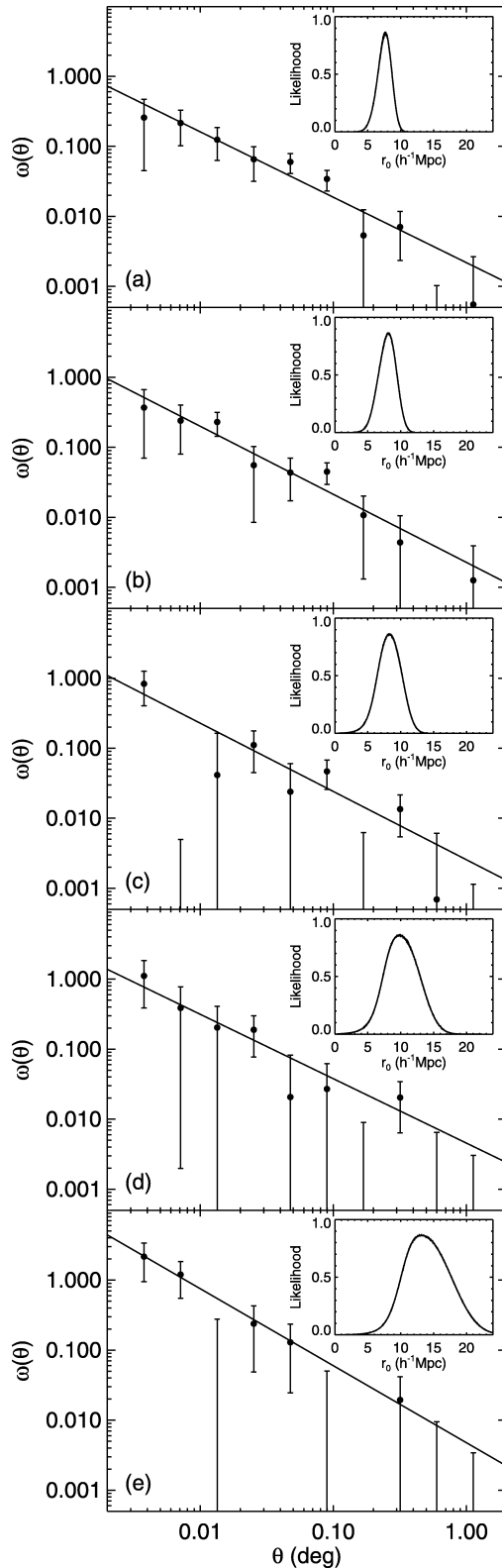

FIG. 1.—Angular correlation functions for (a) the full DOG sample, (b) fainter DOGs with $0.3 \leq F_{24}$ (mJy) < 0.5, and brighter DOGs with (c) $F_{24} >$ 0.4, (d) $F_{24} > 0.5$, and (e) $F_{24} > 0.6$ mJy. The red lines show the best χ^2 fits; the insets show the Bayesian likelihood functions in r_0. All slopes are consistent with $\delta = 0.9$.
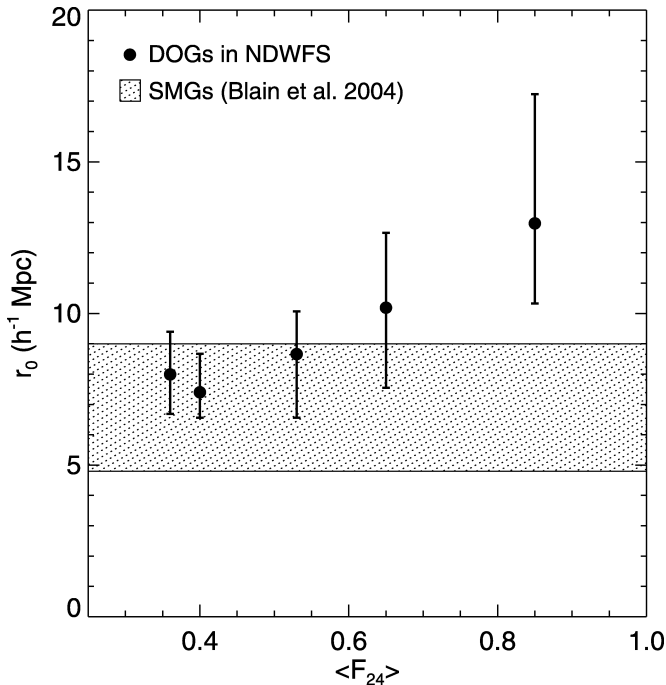
FIG. 2.—Dependence of correlation length on median flux for the samples shown in Fig. 1 and summarized in Table 1, illustrating that clustering strength increases with median luminosity. The shaded region shows the 1 σ range for SMGs (Blain et al. 2004).

If the fainter DOGs are largely star-formation dominated (e.g., D08; P08) they would likely have a narrower redshift distribution due to the strong 7.7 μm PAH emission feature passing through the 24 μm filter at $z = 2$. In this case the evidence for luminosity-dependent clustering would be *strengthened* since the correct correlation length for fainter DOGs would be reduced relative to that of the brighter ones. Quantitatively, if the true redshift distribution were 10% (30%) narrower the correlation lengths would be reduced by 5% (17%).

4. DISCUSSION AND CONCLUSIONS

To similar flux limits ($F_{24} > 0.4$ mJy) the clustering amplitudes measured for other $z \sim 2$ ULIRG samples are higher than those for DOGs in Boötes. In the SWIRE (Lonsdale et al. 2003) survey fields Farrah et al. (2006) find correlation lengths of $r_0 = 9.4 \pm 2.24$ and 14.4 ± 1.99 h^{-1} Mpc for ULIRG samples at $1.5 < z < 2$ and $2 < z < 3$, respectively. In a 0.7 deg^2 subset of the same survey Magliocchetti et al. (2008) find $r_0 = 15.9^{+2.9}_{-3.4}$ h^{-1} Mpc for a sample of 210 $z \sim 2$ ULIRGs. Beyond the fact that the samples in these works have different selection criteria, from each other and from the DOG sample, the most likely explanation for the differences with our work is that they adopt broader redshift distributions based on photometric redshifts. Desai et al. (2008a) and D08 demonstrate that optical/IR photometric redshifts can be unreliable for these heavily obscured sources, particularly when the optical detections are marginal or nonexistent. These previous analyses have likely underestimated their uncertainties, because they fixed the slope of the correlation function, eliminating the covariance between the slope and r_0, and adopted simple Poisson errors, ignoring correlations between adjacent bins.

While DOGs are a mixed population, consisting of both starbursting galaxies and AGN, a majority are dominated by star formation (P08). It is interesting then that the space den-
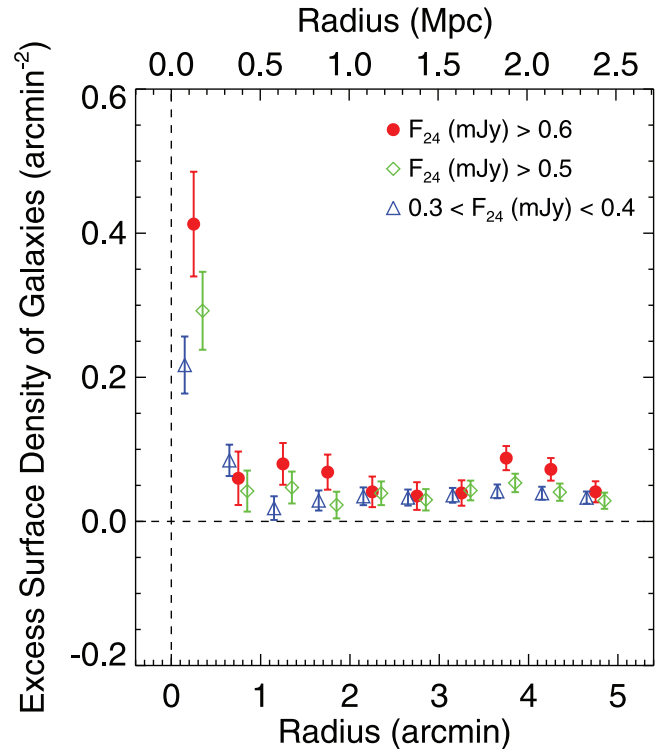

FIG. 3.—Surface profile of $z \gtrsim 1.5$ 4.5 μm sources in Boötes around DOG samples with various flux limits. The contribution from the mean has been subtracted. There is a clear luminosity dependence to the profiles such that brighter DOGs lie in increasingly rich environments. The top axis is in physical separations at $z = 2$ for our chosen cosmology. The region within $\lesssim$250 kpc of the DOGs is particularly rich. Some of the symbols are offset slightly in radius for clarity.

sities (D08) and clustering are quite similar to SMGs (Coppin et al. 2006; Blain et al. 2004), which are known to be star-formation dominated (Pope et al. 2008a).

On the other hand, the AGN fraction increases with luminosity (P08; D08; Tyler et al. 2008). The very strong clustering of brighter DOGs implies they are located in rare, rich environments. Indeed, Galametz et al. (2008) find a strong increase in the incidence of AGN in rich galaxy clusters at $z > 1$. We show in Figure 3 the surface density profiles of 4.5 μm selected galaxies from the IRAC Shallow Survey (Eisenhardt et al. 2004; Brodwin et al. 2006) around DOG samples with several flux limits. We only consider IRAC galaxies with colors redder than $[3.6] - [4.5] > 0.6$, a criterion that selects objects at $z \gtrsim 1.5$ (Stern et al. 2005; Papovich 2008). Following Padmanabhan et al. (2008) the mean space density of these 4.5 μm sources has been subtracted. All DOG samples are clearly correlated with the red IRAC galaxies, showing a large excess on small scales. The mean surface densities of IRAC sources in the vicinity of the DOGs increases monotonically with their brightnesses, indicating that brighter DOGs do in fact reside in richer environments, as suggested by their stronger clustering. The environment of the DOGs is particularly rich on small ($\lesssim$250 kpc) scales, suggesting that they preferentially reside in groups of galaxies. This inference is supported by their large clustering amplitudes, as well as by recent theoretical work (e.g., Hopkins et al. 2008) showing that at $z \sim 2$ the maximal merging efficiency of gas-rich halos, and hence resultant starburst activity, occurs in group-mass halos.

D08 proposed that both types of DOGs are drawn from the

same parent population, and that the luminosity dependence of the AGN fraction arises from the additional energy output from those DOGs undergoing an active AGN phase. The present results suggest an alternative explanation. Although the evidence for luminosity-dependent clustering is marginal given the large errors, the corroborating observation that brighter DOGs reside in richer environments than fainter ones indicates that they are not drawn from identical parent populations. This conclusion is robust to uncertainties in the redshift distribution, provided a single distribution is used for both bright and faint DOG samples. If the redshift distribution of faint DOGs were narrower, the likeliest situation, the strength of the luminosity dependence would increase.

The linear biases of the DOG samples, listed in Table 1, are computed as the square root of the ratio of the $z = 2$ DOG and dark matter correlation functions at a scale of $5\ h^{-1}$ Mpc, where the latter is computed following the HaloFit prescription of Smith et al. (2003). The full sample has a bias of $b = 3.12^{+0.51}_{-0.34}$, where the uncertainty is propagated from the error in the clustering. The bias increases with DOG flux, from $b = 3.36^{+0.56}_{-0.52}$ for faint DOGs ($\langle F_{24} \rangle = 0.36$ mJy) to $b = 5.33^{+1.65}_{-1.04}$ for bright DOGs ($\langle F_{24} \rangle = 0.85$ mJy). Comparison of the observed clustering with that of halos in a large, high-resolution numerical simulation (described in detail in Brown et al. 2008) indicates that the full DOG sample has an average halo mass of $\log M = 12.2^{+0.3}_{-0.2}\ M_\odot$. The masses increase with DOG luminosity, as shown in Table 1, reaching $\log M = 13.0^{+0.4}_{-0.3}$ $M_\odot$ for the brightest DOGs. In the Fry (1996) biased structure formation model, assuming merger-free passive evolution, these samples will evolve into $\approx 3.4 L_*$ and $\approx 6.6 L_*$ galaxies by the present day. The latter have the masses of brightest cluster galaxies in local clusters.

At low redshift the space density and color bimodality of galaxies can be modeled by truncating star formation in galaxies above a particular host halo mass (e.g., Kauffmann et al. 2003; Croton et al. 2006; Brown et al. 2008). Several papers suggest that the transition halo mass is $\sim 10^{12}\ M_\odot$, and this mass

undergoes negligible evolution at $z < 1$ (e.g., Dekel & Birnboim 2006; Cattaneo et al. 2008; Brown et al. 2008). The $z \sim 2$ DOGs, most of which are undergoing vigorous star formation, reside in $\approx 10^{12}$–$10^{13}\ M_\odot$ halos. Perhaps the mode of gas accretion onto massive halos changes at $z > 1$, as suggested by the virial shock heating model of Dekel & Birnboim (2006).

In summary, the DOG sample presented in D08 is a highly clustered population of luminous, obscured galaxies at $z \approx 2$, with $r_0 = 7.40^{+1.27}_{-0.84}\ h^{-1}$ Mpc. Their clustering, space density, and redshift distribution are quite similar to SMGs, indicating that they reside in similar mass halos and suggesting a possible connection between these populations. The clustering strength increases with luminosity, up to $r_0 = 12.97^{+4.26}_{-2.64}\ h^{-1}$ Mpc for $F_{24} > 0.6$ mJy DOGs. Luminous DOGs also reside in richer environments than fainter ones. These results suggest that luminous DOGs, which are more likely to host active AGNs, are not drawn from the same parent population as faint ones, but rather reside in more massive halos. DOGs are highly biased, with $3.1 < b < 5.3$, corresponding to masses of $12.2 < \log (M/M_\odot) < 13.0$ over the luminosity range studied here. They are a population of vigorously star forming galaxies with halo masses larger than $10^{12}\ M_\odot$, the suggested critical mass for the truncation of star formation. They will likely evolve into very massive ($3 \lesssim L/L_* \lesssim 7$) local galaxies.

REFERENCES

Blain, A. W., Chapman, S. C., Smail, I., & Ivison, R. 2004, ApJ, 611, 725
Brand, K., et al. 2007, ApJ, 663, 204
Brodwin, M., Gonzalez, A. H., Moustakas, L. A., Eisenhardt, P. R., Stanford, S. A., Stern, D., & Brown, M. J. I. 2007, ApJ, 671, L93
Brodwin, M., et al. 2006, ApJ, 651, 791
Brown, M. J. I., et al. 2008, ApJ, 682, 937
Caputi, K. I., et al. 2007, ApJ, 660, 97
Cattaneo, A., Dekel, A., Faber, S. M., & Guiderdoni, B. 2008, MNRAS, 389, 567
Chapman, S. C., Blain, A. W., Smail, I., & Ivison, R. J. 2005, ApJ, 622, 772
Coppin, K., et al. 2006, MNRAS, 372, 1621
Croton, D. J., et al. 2006, MNRAS, 365, 11
Dekel, A., & Birnboim, Y. 2006, MNRAS, 368, 2
Desai, V., et al. 2008a, ApJ, 679, 1204
———. 2008b, ApJ, submitted
Dey, A., et al. 2008, ApJ, 677, 943 (D08)
Dickinson, M., Papovich, C., Ferguson, H. C., & Budavári, T. 2003, ApJ, 587, 25
Eisenhardt, P. R., et al. 2004, ApJS, 154, 48
Eisenstein, D. J., & Zaldarriaga, M. 2001, ApJ, 546, 2
Farrah, D., et al. 2006, ApJ, 643, L139
Fiore, F., et al. 2008, ApJ, 672, 94
Fry, J. N. 1996, ApJ, 461, L65

Galametz, A., et al. 2008, ApJ, submitted
Hamilton, A. J. S. 1993, ApJ, 417, 19
Hopkins, P. F., Hernquist, L., Cox, T. J., & Kereš, D. 2008, ApJS, 175, 356
Houck, J. R., et al. 2005, ApJ, 622, L105
Jannuzi, B. T., & Dey, A. 1999, in ASP Conf. Ser. 191, Photometric Redshifts and the Detection of High Redshift Galaxies, ed. R. Weymann et al. (San Francisco: ASP), 111
Kauffmann, G., et al. 2003, MNRAS, 341, 54
Landy, S. D., & Szalay, A. S. 1993, ApJ, 412, 64
Le Floc'h, E., et al. 2005, ApJ, 632, 169
Limber, D. N. 1954, ApJ, 119, 655
Lonsdale, C. J., et al. 2003, PASP, 115, 897
Magliocchetti, M., et al. 2008, MNRAS, 383, 1131
Padmanabhan, N., White, M., Norberg, P., & Porciani, C. 2008, MNRAS, submitted (arXiv:0802.2105)
Papovich, C. 2008, ApJ, 676, 206
Pope, A., et al. 2008a, ApJ, 675, 1171
———. 2008b, ApJ, in press (P08)
Rudnick, G., et al. 2006, ApJ, 650, 624
Smith, R. E., et al. 2003, MNRAS, 341, 1311
Stern, D., et al. 2005, ApJ, 631, 163
Tyler, K. D., et al. 2008, ApJ, submitted
Weedman, D. W., et al. 2005, ApJ, 633, 706